Inorg. Chem. **2008**, *47*, 5225−5233

Hydrothermal Reaction of Cu(II)/Pyrazine-2,3,5-tricarboxylic acid and Characterization of the Copper(II) Complexes

Feng-Qin Wang,[†,‡] Wei-Hua Mu,[†] Xiang-Jun Zheng,[†] Li-Cun Li,[§] De-Cai Fang,*[,†] and Lin-Pei Jin*[,†]

Department of Chemistry, Beijing Normal University, Beijing 100875, P.R. China, Faculty of Materials Science & Engineering, Tianjin Polytechnic University, Tianjin 300160, P.R. China, and Department of Chemistry, Nankai University, Tianjin 300071, P.R. China

Received February 1, 2008

Four copper(II) complexes $[Cu_3(PZHD)_2(2,2'\text{-bpy})_2(H_2O)_2]\cdot 3H_2O$ (**1**), $[Cu_3(DHPZA)_2(2,2'\text{-bpy})_2]$ (**2**), $[Cu(C_2O_4)\text{-phen}(H_2O)]\cdot H_2O$ (**3**), and $[Cu_3(PZTC)_2(2,2'\text{-bpy})_2]\cdot 2H_2O$ (**4**) were synthesized by hydrothermal reactions, in which the complexes **1**−**3** were obtained by the in situ Cu(II)/H_3PZTC reactions ($PZHD^{3-}$ = 2-hydroxypyrazine-3,5-dicarboxylate, 2,2′-bpy = 2,2′-bipyridine, $DHPZA^{3-}$ = 2,3-dihydroxypyrazine-5-carboxylate, $C_2O_4^{2-}$ = oxalate, phen = 1,10-phenanthroline, and H_3PZTC = pyrazine-2,3,5-tricarboxylic acid). The Cu(II)/H_3PZTC hydrothermal reaction with 2,2′-bpy, without addition of NaOH, results in the formation of complex **4**. The complexes **1**−**4** and transformations from H_3PZTC to $PZHD^{3-}$, $DHPZA^{3-}$, and $C_2O_4^{2-}$ were characterized by single-crystal X-ray diffraction and theoretical calculations. In the complexes **1**, **2**, and **4**, the ligands $PZHD^{3-}$, $DPHZA^{3-}$, and $PZTC^{3-}$ all show pentadentate coordination to Cu(II) ion forming three different trinuclear units. The trinuclear units in **1** are assembled by hydrogen-bonding and π-π stacking to form a 3D supramolecular network. The trinuclear units in **2** acting as building blocks are connected by the carboxylate oxygen atoms forming a 2D metal-organic framework (MOF) with (4,4) topology. While the trinuclear units in **4** are linked together by the carboxylate oxygen atoms to form a novel 2D MOF containing right- and left-handed helical chains. The theoretical characterization testifies that electron transfer between OH^- and Cu^{2+} and redox of Cu^{2+} and Cu^+ are the most important processes involved in the in situ copper Cu(II)/H_3PZTC reactions, forming complexes of **1**−**3**.

Introduction

Hydro- and solvo-thermal in situ metal/ligand reactions which feature chemical reactions in a sealed solution at elevated temperature and autogenous pressure have been an active research field in both coordination chemistry and synthetic organic chemistry.[1] The most attractive of the in situ metal/ligand reactions is used as a powerful technique for the synthesis of new organic compounds and coordination compounds. This method has been extensively applied in the construction of metal-organic frameworks (MOFs) which show unique structural diversity and promising physical/chemical properties for potential applications in the past twenty years.[2] Li and coauthors first published hydrothermal in situ ligand reactions in 1998 on the rearrangement of 2,2′-bipyridylamine into dipyrido-[1,2-a:2′,3′-d]imidazole in the synthesis of $_\infty^1[(CuCl)_2(C_{10}H_7N_3)]$ and $_\infty^1[(CuBr)_3(C_{10}H_7N_3)]$.[3] Late in the same year, Liu and coauthors reported in situ metal/nitrile reactions for the synthesis of chiral and acentric NLO-active 2D polymeric metal-organic coordination networks.[4] Since then many kinds of in situ metal/ligand reactions have been explored.[1] Often such reactions include

* To whom correspondence should be addressed. E-mail: lpjin@bnu.edu.cn.
† Beijing Normal University.
‡ Tianjin Polytechnic University.
§ Nankai University.

(1) (a) Chen, X. M.; Tong, M. L. *Acc. Chem. Res.* **2007**, *40*, 162–170. (b) Zhang, X,M. *Coord. Chem. Rev.* **2005**, *249*, 1201.
(2) (a) Zhang, X. M.; Tong, M. L.; Chen, X. M. *Angew. Chem., Int. Ed.* **2002**, *41*, 1029. (b) Evans, O. R.; Lin, W. B. *Chem. Mater.* **2001**, *13*, 2705. (c) Xiong, R. G.; Xue, X.; Zhao, H.; You, X. Z.; Abrahams, B. F.; Xue, Z. *Angew. Chem., Int. Ed.* **2002**, *41*, 3800. (d) Chen, W.; Yuan, H. M.; Wang, J. Y.; Liu, Z. Y.; Xu, J. J.; Yang, M.; Chen, J. S. *J. Am. Chem. Soc.* **2003**, *125*, 9266.
(3) Lu, J. Y.; Cabrera, B. R.; Wang, R. J.; Li, J. *Inorg. Chem.* **1998**, *37*, 4480.
(4) Lin, W. B.; Evans, O. R.; Xiong, R. G.; Wang, Z. *J. Am. Chem. Soc.* **1998**, *120*, 13272.

10.1021/ic8001916 CCC: $40.75
Published on Web 05/20/2008

decarboxylation of aromatic carboxylates.[5] Jao et al. reported the first example of hydroxylation of aromatic carboxylic acid in the situ synthesis of copper 2-hydroxyisophthalate complex under the hydrothermal reaction of isophthalate and 4,4′-bipyridine with $Cu(NO_3)_2 \cdot 3H_2O$.[6] Although the carboxylate groups of carboxylic acids could have been released or replaced under hydrothermal conditions, the formation of oxalate from carboxylate groups of aromatic carboxylic acid under hydrothermal conditions is intriguing.[7] Evidently such reactions require further understanding. We reported the in situ Cu(II)/pyrazine-2,3-dicarboxylic acid hydrothermal reaction. A new ligand and two new Cu(II) complexes are formed, which are theoretically characterized.[8] This work reports the synthesis and structure of the copper(II) complexes obtained from the Cu(II)/pyrazine-2,3,5-tricarboxylic acid reaction under hydrothermal conditions at different temperatures and pHs. Especially we describe the mechanism of the conversion from aromatic tricarboxylic acid to hydroxypyrazinedicarboxylate, dihydroxypyrazinecarboxylate, and oxalate, and thus the formation mechanism of the copper(II) complexes has been characterized by theoretical calculation.

Experimental Section

Materials and Physical Measurements. Pyrazine-2,3,5-tricarboxylic acid dihydrate was synthesized according to the literature.[9] All the other reagents were used as received without further purification. The C, H, N microanalyses were carried out with a Vario EL elemental analyzer. The IR spectra were recorded with a Nicolet Avatar 360 FT-IR spectrometer using the KBr pellet technique. Variable temperature magnetic susceptibility data of complexes **1**, **2**, and **4** were measured on a MagLab System 2000 in the 2−300K range under the applied magnetic field of 2000 G. Diamagnetic corrections were made with Pascal's constants for all the constituent atoms. Experimental susceptibilities were also corrected for the temperature-independent paramagnetism (60×10^{-6} cm^3 mol^{-1} per Cu(II)) and the magnetization of the sample holder.

Synthesis of $[Cu_3(PZHD)_2(2,2'\text{-bpy})_2(H_2O)_2] \cdot 3H_2O$ (1). A mixture of H_3PZTC (0.025 g, 0.1 mmol), $Cu(Ac)_2 \cdot 2H_2O$ (0.030 g, 0.15 mmol), 2,2′-bpy (0.0234 g, 0.15 mmol), NaOH (0.45 mL, 0.65 $mol \cdot L^{-1}$), and H_2O (5 mL) was put into a 25 mL stainless steel bomb and heated at 100° for 4 days, then cooled to room temperature. Green plate crystals were obtained by filtration. Yield: 72.2% based on Cu. Elemental analysis (%) calcd for $C_{32}H_{28}Cu_3N_8O_{15}$: C 40.23, H 2.95, N 11.73. Found: C 40.31, H 3.07, N 11.40. IR data (KBr pellet, cm^{-1}): 3419 br, 1602 vs, 1507 s, 1446 m, 1390 m, 1350 m, 1318 s, 1218 m, 1199 m, 1034 w, 975 w, 827 w, 774 m.

$[Cu_3(DHPZA)_2(2,2'\text{-bpy})_2]$ (2). Complex **2** was obtained by a procedure similar to that for **1** but only changing the reaction temperature from 100 to 140 °C. Dark blue plate crystals suitable for X-ray diffraction were separated by filtration. Yield: 70.4% based on Cu. Elemental analysis (%) calcd for $C_{30}H_{18}Cu_3N_8O_8$: C 44.49, H 2.22, N 13.84. Found: C 43.99, H 2.96, N 13.55. IR(KBr pellet, cm^{-1}): 3441 br, 1606 s, 1541 s, 1484 s, 1400 m, 1346 s, 1319 s, 1205 m, 1148 w, 1053 m, 1035 w, 810 m, 779 m.

$[Cu(C_2O_4)(phen)(H_2O)] \cdot H_2O$ (3). A mixture of H_3PZTC (0.0190 g, 0.075 mmol), $Cu(NO_3)_2 \cdot 2H_2O$ (0.072 g, 0.3 mmol), phen(0.078 g, 0.39 mmol), NaOH (0.35 mL, 0.65 $mol \cdot L^{-1}$), and H_2O (6 mL) was put into a 25 mL stainless steel bomb and heated at 140° for 4 days. Dark green plate crystals were obtained by filtration. Yield: 57.1% based on Cu. Elemental analysis (%) calcd for $C_{14}H_{12}CuN_2O_6$: C 41.97, H 3.96, N 12.24. Found: C 42.36, H 4.05, N 12.32. IR (KBr pellet, cm^{-1}): 3415 br, 1633 s, 1602 m, 1573 m, 1446 s, 1355 s, 1183 m, 1053 m, 1032 w, 790 m.

$[Cu_3(PZTC)_2(2,2'\text{-bpy})_2] \cdot 2H_2O$ (4). Complex **4** was obtained by a procedure similar to that for **2** only in the absence of NaOH. Bluish-green plate crystals were obtained by filtration. Yield: 68.9% based on Cu. Elemental analysis (%) calcd for $C_{34}H_{22}Cu_3N_8O_{14}$: C 42.62, H 2.30, N 11.70. Found: C 42.11, H 2.51, N 11.71. IR (KBr pellet, cm^{-1}): 3415 br, 1662 vs, 1635 vs, 1501 w, 1467 w, 1446 m, 1438 m, 1399 m, 1335 s, 1297 s, 1204 m, 1184 s, 1097 m, 851 m, 774 m.

X-ray Structure Determination. Diffraction intensities for complexes **1**−**4** were collected at 293 K on a computer-controlled Bruker SMART 1000 CCD diffractometer equipped with graphite-monochromated Mo Kα radiation with a radiation wavelength of 0.71073 Å by using the ω-φ scan technique. Lorentz polarization and absorption corrections were applied. The structures were solved by direct methods and refined with the full-matrix least-squares technique using the SHELXS 97 and SHELXL 97 programs.[10] Anisotropic thermal parameters were assigned to all non-hydrogen atoms. The hydrogen atoms were set in calculated positions and refined as riding atoms with a common fixed isotropic thermal parameter.

Computational Methods. Density Functional Theory (DFT)[11] calculations employing the SCRF-UB3LYP/6−31+G(d)[12] method (LANL2DZ[13] for Cu atoms) have been carried out to characterize the formation mechanisms of complexes **1**−**4**, in which the Polarized Continuum Model (PCM)[14] and water as solvent have been used for simulating the real experimental conditions. The geometric parameters of all attempted stationary points have

(5) (a) Zheng, Y. Z.; Tong, M. L.; Chen, X. M. *New J. Chem.* **2004**, *28*, 1412. (b) Li, X. J.; Cao, R.; Guo, Z. G.; Lü, J. *Chem. Commun.* **2006**, 1938. (c) Lu, J. Y.; Bahh, A. M. *Inorg. Chem.* **2002**, *41*, 1339.

(6) Jao, J.; Zhang, Y.; Tong, M. L.; Chen, X. M.; Yuen, T.; Liu, C. L.; Huang, X. Y.; Li, J. *Chem. Commun.* **2002**, 1342.

(7) (a) Orioli, P.; Bruni, B.; Varia, M. D.; Messori, L.; Piccioli, F. *Inorg. Chem.* **2002**, *41*, 4312. (b) Li, B.; Gu, W.; Zhang, L. Z.; Qu, J.; Ma, Z. P.; Liu, X.; Liao, D. Z. *Inorg. Chem.* **2006**, *45*, 10425.

(8) Weng, D. F.; Mu, W. H.; Zheng, X. J.; Fang, D. C.; Jin, L. P. *Inorg. Chem.* **2008**, *47*, 1249.

(9) (a) Mager, H. I. X.; Berends, W. *Recl. Trav. Chim. Pays-Bas* **1958**, *77*, 827. (b) Weygand, F. *Chem. Ber.* **1940**, *73*, 1259. (c) Weygand, F.; Bergmann, C. *Chem. Ber.* **1947**, *80*, 255.

(10) (a) Sheldrick, G. M. *SHELXS 97, Program for Crystal Structure Solution*; University of Göttingen: Göttingen, Germany, 1997. (b) Sheldrick, G. M. *SHELXL 97, Program for Crystal Structure Refinement*, University of Göttingen: Göttingen, Germany, 1997.

(11) (a) Becke, A. D. *J. Chem. Phys.* **1993**, *98*, 5648. (b) Lee, C.; Yang, W.; Parr, R. G. *Phys. Rev. B* **1988**, *37*, 785.

(12) (a) Hariharan, P. C.; Pople, J. A. *Theor. Chim. Acta* **1973**, *28*, 213. (b) Francl, M. M.; Petro, W. J.; Hehre, W. J.; Binkley, J. S.; Gordon, M. S.; DeFrees, D. J.; Pople, J. A. *J. Chem. Phys.* **1982**, *77*, 3654. (c) Krishnam, R.; Binkley, J. S.; Seeger, R.; Pople, J. A. *J. Chem. Phys.* **1980**, *72*, 650. (d) Gill, P. M. W.; Johnson, B. G.; Pople, J. A.; Frisch, M. J. *Chem. Phys. Lett.* **1992**, *197*, 499.

(13) (a) Hay, P. J.; Wadt, W. R. *J. Chem. Phys.* **1985**, *82*, 270. (b) Wadt, W. R.; Hay, P. J. *J. Chem. Phys.* **1985**, *82*, 284. (c) Hay, P. J.; Wadt, W. R. *J. Chem. Phys.* **1985**, *82*, 299.

(14) (a) Miertus, S.; Scrocco, E.; Tomasi, J. *Chem. Phys.* **1981**, *55*, 117. (b) Cossi, M.; Barone, V.; Cammi, R.; Tomasi, J. *Chem. Phys. Lett.* **1996**, *255*, 327. (c) Barone, V.; Cossi, M. *J. Phys. Chem. A* **1998**, *102*, 1995.

Scheme 1. Simplified Routes of Syntheses for the Complexes **1**−**4**

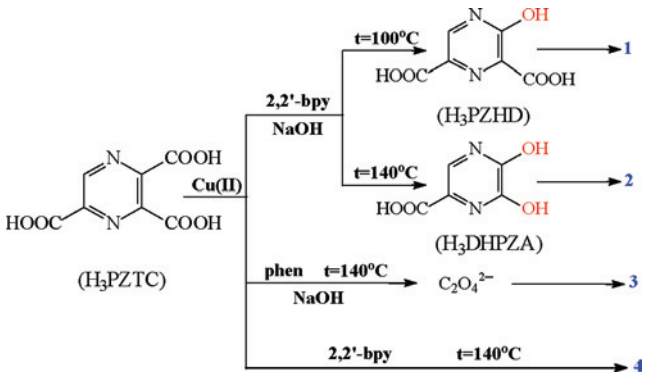

been located and characterized by the number of imaginary frequencies, as implemented in the Gaussian 03 program package.[15] The default convergence criteria are used in the optimization processes, except for what is noted elsewhere. For some selected reaction paths, the Intrinsic Reaction Coordinate (IRC)[16] has been traced to confirm that the transition state (TS) structures obtained correspond to the two minima proposed as lying on either side of that TS. The relative energies of all stationary points have been corrected with zero-point vibrational energies (ZPE), using a scaling factor of 0.96.[17]

For manageable calculations, the auxiliary ligands and copper atoms that would not affect the reaction mechanisms much were omitted to achieve optimization, that is, all of the optimizations were made to find out the formation mechanisms for the corresponding ionic species of compounds H_2PZHD^{1-}, $HDHPZA^{2-}$, H_3PZTC, and $C_2O_4^{2-}$, as shown in Scheme 1.

Results and Discussion

Synthesis. As shown in Scheme 1, complexes **1**, **2**, and **3** were obtained by the in situ Cu(II)/H_3PZTC reaction with different auxiliary ligands 2,2′-bpy (**1** and **2**) and phen (**3**) under hydrothermal conditions. In the 2,2′-bpy system, when the temperature was 100 °C and in the presence of Cu(II) at pH = 5, the H_3PZTC ligand was converted into 2-hydroxypyrazine-3,5-dicarboxylate ($PZHD^{3-}$) by decarboxylation and hydroxylation, which is further assembled into complex **1**. In a similar procedure except that the temperature rose to 140 °C, the H_3PZTC ligand was changed to 2,3-dihydroxypyrazine-5-carboxylate ($DHPZA^{3-}$) which coordinates with Cu(II) ion to form complex **2**. Instead of 2,2′-bpy by phen, the synthetic temperature was 140 °C at pH = 6, H_3PZTC was converted into oxalate, and thus complex **3** was obtained. When the temperature was the same as that for complex **2** and no NaOH was added to the reaction mixture, complex **4** was obtained, which is the first example of transition metal complexes with a H_3PZTC ligand.

The results indicate that the formation of the complexes **1**−**4** shows significant dependence on temperature and addition of NaOH. Higher temperature and pH favor the in situ Cu(II)/H_3PZTC reaction. In **1** and **2**, H_3PZTC can be converted to 2-hydroxypyrazine-3,5-dicarboxylic acid and 2,3-dihydroxypyrazine-5-carboxylic acid, which have not been prepared in organic synthesis yet, showing that the in situ metal/ligand reaction acts as a bridge between coordination chemistry and organic synthesis.

Structural Description. The complex **3** was reported by Cheng et al. in 2001, which was obtained from evaporation of $K_2[Cu(C_2O_4)_2]\cdot 2H_2O$ and 1,10-phenanthroline in ethanol solution.[18] Therefore, we describe structures of the complexes **1**, **2**, and **4**. Crystal data and structure refinement parameters of the complexes **1**−**4** are given in Table 1. The selected bond distances (Å) and angles (deg) are tabulated in Table 2.

$[Cu_3(PZHD)_2(2,2'\text{-bpy})_2(H_2O)_2]\cdot 3H_2O$ (1). Single-crystal X-ray diffraction analysis reveals that **1** is a trinuclear Cu(II) complex. There are three crystallographically independent Cu centers in the asymmetric unit (see Figure 1). Cu2 is six-coordinated with four oxygen atoms and two nitrogen atoms from two PZHD ligands, displaying a distorted octahedral coordination environment. Different from Cu2, both Cu1 and Cu3 are five- coordinated to two oxygen atoms from one PZHD ligand and one oxygen atom from a water molecule, two nitrogen atoms from one 2,2′-bpy molecule, resulting in a distorted square-pyramidal geometry.

In complex **1**, each $PZHD^{3-}$ ligand adopts a pentadentate mode to bind two Cu(II) ions (see Scheme 2a), forming a trinuclear unit (see Figure 1) in which the two $PZHD^{3-}$ ligands are coordinated to Cu2 with a dihedral angle of 69.9° between two pyrazine rings. The separations of Cu1···Cu2 and Cu2···Cu3 are 5.681Å and 5.696Å, respectively. These trinuclear units are assembled by hydrogen bonds between the coordinated water molecules and the carboxylate oxygen atoms or the uncoordinated pyrazine nitrogen atoms and by π-π stacking interactions between the 2,2′-bpy molecules with the distance of 3.440 Å forming a 3D supramolecular network. Figure 2 shows the hydrogen bonding and π-π stacking interactions.

$[Cu_3(DHPZA)_2(2,2'\text{-bpy})_2]$ (2). The complex **2** crystallizes in the space group $P4_12_12$, which has a 2D MOF. In the asymmetric unit, there are two crystallographically independent Cu(II) ions (see Figure 3). Cu1 is four-coordinated with two oxygen atoms and two nitrogen atoms from two $DHPZA^{3-}$ ligands, displaying ideal tetrahedral geometry. The Cu2 is five-coordinated to three oxygen atoms from two $DHPZA^{3-}$ ligands

(15) Frisch, M. J.; Trucks, G. W.; Schlegel, H. B.; Scuseria, G. E.; Robb, M. A.; Cheeseman, J. R.; Montgomery, J. A., Jr.; Vreven, T.; Kudin, K. N.; Burant, J. C.; Millam, J. M.; Iyengar, S. S.; Tomasi, J.; Barone, V.; Mennucci, B.; Cossi, M.; Scalmani, G.; Rega, N.; Petersson, G. A.; Nakatsuji, H.; Hada, M.; Ehara, M.; Toyota, K.; Fukuda, R.; Hasegawa, J.; Ishida, M.; Nakajima, T.; Honda, Y.; Kitao, O.; Nakai, H.; Klene, M.; Li, X.; Knox, J. E.; Hratchian, H. P.; Cross, J. B.; Adamo, C.; Jaramillo, J.; Gomperts, R.; Stratmann, R. E.; Yazyev, O.; Austin, A. J.; Cammi, R.; Pomelli, C.; Ochterski, J. W.; Ayala, P. Y.; Morokuma, K.; Voth, G. A.; Salvador, P.; Dannenberg, J. J.; Zakrzewski, V. G.; Dapprich, S.; Daniels, A. D.; Strain, M. C.; Farkas, O.; Malick, D. K.; Rabuck, A. D.; Raghavachari, K.; Foresman, J. B.; Ortiz, J. V.; Cui, Q.; Baboul, A. G.; Clifford, S.; Cioslowski, J.; Stefanov, B. B.; Liu, G.; Liashenko, A.; Piskorz, P.; Komaromi, I.; Martin, R. L.; Fox, D. J.; Keith, T.; Al-Laham, M. A.; Peng, C. Y.; Nanayakkara, A.; Challacombe, M., Gill, P. M. W.; Johnson, B.; Chen, W.; Wong, M. W.; Gonzalez, C.; Pople, J. A. *Gaussian 03*, Revision C.02; Gaussian, Inc.: Wallingford, CT, 2004.
(16) (a) Gonzalez, C.; Schlegel, H. B. *J. Chem. Phys.* **1989**, *90*, 2154. (b) Gonzalez, C.; Schlegel, H. B. *J. Phys. Chem.* **1990**, *94*, 5523.
(17) Scott, A. P.; Radom, L. *J. Phys. Chem.* **1996**, *100*, 16502.
(18) Chen, X, F.; Cheng, P.; Liu, X.; Zhao, B.; Liao, D. Z.; Yan, S. P.; Jiang, Z. H. *Inorg. Chem.* **2001**, *40*, 2652.

Table 1. Crystal Data and Structure Refinement Parameters of the Complexes **1**−**4**

	1	**2**	**3**	**4**
chemical formula	$C_{32}H_{28}Cu_3N_8O_{15}$	$C_{30}H_{18}Cu_3N_8O_8$	$C_{14}H_{12}CuN_2O_6$	$C_{34}H_{22}Cu_3N_8O_{14}$
formula weight	955.24	809.14	367.80	957.22
temperature (K)	294(2)	293(2)	294(2)	294(2)
crystal system	triclinic	tetragonal	monoclinic	monoclinic
space group	$P\bar{1}$	$P4_12_12$	$P2_1/n$	$P2_1/c$
a (Å)	8.563(4)	8.617(6)	8.466(12)	9.556(11)
b (Å)	12.248(5)	8.617(6)	9.709(14)	17.521(3)
c (Å)	16.987(7)	37.986(5)	17.46(3)	10.064(16)
α (°)	81.076(7)	90	90	90
β (°)	84.387(7)	90	103.88(2)	90.821(5)
γ (°)	85.820(8)	90	90	90
V (Å^3)	1748.6(13)	2820.8(4)	1392.9(4)	1684.9(4)
Z	2	4	4	2
F (000)	966	1620	748	962
ρ [mg m^{-3}]	1.814	1.905	1.754	1.887
μ [mm^{-1}]	1.895	2.313	1.603	1.965
θ range (deg)	1.22−25.01	2.14−26.39	2.40−26.38	2.13−27.87
no. collected data	8967	15925	7667	12814
no. unique data, R_{int}	6118, 0.0461	2886, 0.0457	2838, 0.0327	3839, 0.0282
GOF	0.990	1.073	1.035	1.036
R indices [$I > 2\sigma(I)$]	$R_1 = 0.0507$	$R_1 = 0.0370$	$R_1 = 0.0295$	$R_1 = 0.0308$
	$wR_2 = 0.0965$	$wR_2 = 0.0822$	$wR_2 = 0.0725$	$wR_2 = 0.0773$
R indices (all data)	$R_1 = 0.1163$	$R_1 = 0.0446$	$R_1 = 0.0440$	$R_1 = 0.0380$
	$wR_2 = 0.1234$	$wR_2 = 0.0849$	$wR_2 = 0.0795$	$wR_2 = 0.0824$

and two nitrogen atoms from one 2,2′-bpy molecule displaying a distorted square pyramid geometry.

In complex **2**, each $DHPZA^{3-}$ ligand adopts a pentadentate mode to link three Cu(II) ions. Its coordination mode is shown in Scheme 2b: two hydroxyl oxygen atoms bind one Cu(II) ion, one pyrazine nitrogen atom together with one neighboring carboxylate oxygen atom coordinate the second Cu(II) ion, and the remaining oxygen atom of the carboxylate group links the third Cu(II) ion. In this way, the $DHPZA^{3-}$ ligands link the metal ions to form a trinuclear unit. These trinuclear units acting as the building blocks are connected by carboxylate oxygen atoms forming 2D MOFs with a 32-membered metallocycle. In the 2D structure, Cu(II) ions lie in three different planes and form a (4,4) topology layer (see Figure 4a). Figure 4b shows that Cu(II) ions locate at three different layers. The complex has 4_1 helix and the angle between the neighboring layers is 90°. Along the *c*-axis direction, these 2D layers are further stacked by hydrogen bonds (C−H···O) forming a supramolecular network.

$[Cu_3(PZTC)_2(2,2'\text{-bpy})_2]\cdot 2H_2O$ (4). In the asymmetric unit of **4**, there are two crystallographically independent Cu(II) ions (see Figure 5). Cu1 is five-coordinated with two oxygen atoms and one nitrogen atom from two $PZTC^{3-}$ ligands, and two nitrogen atoms from one 2,2′-bpy molecule, displaying a distorted square pyramid geometry. Cu2 is four-coordinated to two oxygen atoms and two nitrogen atoms from two $PZTC^{3-}$ ligands, displaying square planar coordination geometry. The Cu2−O and Cu2−N bond lengths are all 1.962(2)Å.

In complex **4**, each $PZTC^{3-}$ ligand adopts a pentadentate mode (see Scheme 2c) through its three carboxylate oxygen atoms and two nitrogen atoms to link Cu(II) ions to form a linear trinuclear entity, in which the Cu2 is in the inversion center with Cu1···Cu2 and Cu2···Cu1A separations of 7.053 Å. These trinuclear units acting as the building blocks are linked together by the carboxylate oxygen atoms to form a 2D MOF with a rhombic-grid containing left- and right-hand helical chains (see Figure 6). In the 2D layer, Cu(II) ions are in three different planes, and the adjacent layers are connected via hydrogen bonds between the water molecules located in the void and the carboxylate oxygen atoms from the framework to form a 3D supramolecular network (see Figure 7).

Formation Mechanisms of Complexes 1−4. To characterize the mechanisms for the formation of complexes **1**−**4**, DFT calculations employing the SCRF-UB3LYP/6−31+G(d) method (where the LANL2DZ basis set was used for Cu atoms) have been carried out. To test the reliability of the method employed in our calculation, the optimized geometric parameters at SCRF-UB3LYP/6−31+G(d) level for the structures that lead to complexes **1**−**4** are depicted in Figure 8, along with those of the crystal data in parentheses.

The obtained results demonstrate that the optimized geometric parameters for most of the Cu−O and Cu−N bonds (except for Cu1−N1 bond in **INT1Cu**) are close to the corresponding ones in the crystal structures. Further optimization about intermediate **INT1Cu**, with Cu1 set in a similar coordination environment to complex **4**, indicates that the difference between the computed and crystal data becomes only ∼0.05 Å. Actually, it is very hard to optimize such structures with auxiliary ligands because it involves so many coordinates, especially the rotations of some loose coordinated bonds. For a manageable approach, the auxiliary ligands could be omitted, which is confirmed in our previous work.[8]

As shown in Figure 9, the reactant H_3PZTC (**R1**) loses its three acid hydrogen atoms to form the anionic **INT1** ($PZTC^{3-}$), which coordinates with Cu^{2+} ion to form **INT1Cu**. **INT1Cu** can be crystallized to form crystal **4** with the participation of Cu^{2+} coordinating with the ligand 2,2′-bpy. **INT1Cu** can also be transformed to **INT2Cu** via a transition state **TS1Cu** with a very small activation energy barrier of ∼0.7 kcal/mol; thus, **INT2Cu** generated could easily form **COM1Cu** with the attack of OH^-, with an energy release of ∼21.4 kcal/mol. **COM1Cu** can be further

Table 2. Selected Bond Lengths (Å) and Angles of Complexes **1**, **2**, and **4**

	Complex **1**		
Cu(1)−O(1)	2.236(5)	Cu(2)−O(3)	2.127(4)
Cu(1)−O(4)	1.905(4)	Cu(2)−O(5)	2.115(4)
Cu(1)−N(1)	1.998(5)	Cu(2)−O(7)	2.273(4)
Cu(1)−O(2)	1.945(4)	Cu(2)−O(9)	2.264(5)
Cu(1)−N(2)	1.991(5)	Cu(2)−N(3)	1.918(5)
Cu(2)−N(5)	1.952(5)	Cu(3)−O(10)	1.915(4)
Cu(3)−O(11)	1.927(4)	Cu(3)−O(12)	2.375(4)
Cu(3)−N(8)	1.997(5)	Cu(3)−N(7)	1.990(5)
O(2)−Cu(1)−O(1)	94.45(18)	O(2)−Cu(1)−N(1)	92.08(18)
O(2)−Cu(1)−N(2)	167.0(2)	O(4)−Cu(1)−O(1)	98.06(18)
O(4)−Cu(1)−O(2)	95.33(16)	O(4)−Cu(1)−N(1)	167.5(2)
O(4)−Cu(1)−N(2)	89.5(2)	N(1)−Cu(1)−O(1)	91.34(19)
N(2)−Cu(1)−O(1)	96.90(19)	N(2)−Cu(1)−N(1)	81.3(2)
O(3)−Cu(2)−O(7)	84.70(16)	O(3)−Cu(2)−O(9)	100.58(16)
O(5)−Cu(2)−O(3)	157.76(15)	O(5)−Cu(2)−O(7)	99.68(16)
O(9)−Cu(2)−O(7)	152.74(15)	O(5)−Cu(2)−O(9)	85.54(17)
N(3)−Cu(2)−O(3)	78.49(17)	N(3)−Cu(2)−O(5)	79.50(18)
N(3)−Cu(2)−O(7)	109.35(18)	N(3)−Cu(2)−O(9)	97.91(18)
N(5)−Cu(2)−O(3)	102.66(16)	N(5)−Cu(2)−O(5)	99.56(17)
N(5)−Cu(2)−O(7)	76.62(18)	N(5)−Cu(2)−O(9)	76.13(18)
N(3)−Cu(2)−N(5)	174.0(2)	O(10)−Cu(3)−O(11)	94.28(18)
O(10)−Cu(3)−O(12)	94.65(18)	O(10)−Cu(3)−N(7)	168.8(2)
O(10)−Cu(3)−N(8)	90.2(2)	O(11)−Cu(3)−O(12)	93.94(18)
O(11)−Cu(3)−N(7)	92.8(2)	O(11)−Cu(3)−N(8)	168.3(2)
N(7)−Cu(3)−O(12)	93.54(17)	N(7)−Cu(3)−N(8)	81.3(2)
N(8)−Cu(3)−O(12)	96.45(18)		
	Complex **2**[a]		
Cu(1)−O(1)	1.942(3)	Cu(2)−O(2)#2	2.393(3)
Cu(1)−O(1)#1	1.942(3)	Cu(2)−O(3)	1.944(3)
Cu(1)−N(1)	1.942(3)	Cu(2)−O(4)	1.932(3)
Cu(1)−N(1)#1	1.942(3)	Cu(2)−N(3)	1.975(3)
		Cu(2)−N(4)	2.000(3)
O(1)#1−Cu(1)−O(1)	97.35(16)	O(3)−Cu(2)−N(4)	165.12(13)
O(1)#1−Cu(1)−N(1)	148.55(13)	O(4)−Cu(2)−O(2)#2	100.87(11)
O(1)#1−Cu(1)−N(1)#1	84.09(12)	O(4)−Cu(2)−O(3)	85.78(11)
N(1)−Cu(1)−O(1)	84.08(12)	O(4)−Cu(2)−N(3)	169.44(13)
N(1)#1−Cu(1)−O(1)	148.56(13)	O(4)−Cu(2)−N(4)	96.33(12)
N(1)#1−Cu(1)−N(1)	110.77(18)	N(3)−Cu(2)−O(2)#2	89.52(12)
O(3)−Cu(2)−O(2)#2	102.47(11)	N(3)−Cu(2)−N(4)	81.35(13)
O(3)−Cu(2)−N(3)	93.88(13)	N(4)−Cu(2)−O(2)#2	91.63(12)
	Complex **4**[b]		
Cu(1)−O(1)	1.947(1)	Cu(2)−O(6)	1.962(1)
Cu(1)−O(3)#1	1.965(2)	Cu(2)−O(6)#2	1.962(1)
Cu(1)−N(1)	2.425(2)	Cu(2)−N(2)	1.962(2)
Cu(1)−N(3)	2.010(2)	Cu(2)−N(2)#2	1.962(2)
Cu(1)−N(4)	1.978(2)		
O(1)−Cu(1)−O(3)#1	93.96(6)	N(3)−Cu(1)−N(1)	97.68(6)
O(1)−Cu(1)−N(4)	173.78(7)	N(4)−Cu(1)−N(1)	101.37(6)
O(3)#1−Cu(1)−N(4)	92.16(7)	O(6)#2−Cu(2)−O(6)	180.00(8)
O(1)−Cu(1)−N(3)	93.33(7)	O(6)#2−Cu(2)−N(2)	97.52(6)
O(3)#1−Cu(1)−N(3)	162.96(7)	O(6)−Cu(2)−N(2)	82.48(6)
N(4)−Cu(1)−N(3)	81.07(7)	O(6)#2−Cu(2)−N(2)#2	82.48(6)
O(1)−Cu(1)−N(1)	76.58(5)	O(6)−Cu(2)−N(2)#2	97.52(6)
O(3)#1−Cu(1)−N(1)	98.98(6)	N(2)−Cu(2)−N(2)#2	180.0

[a] #1, $-y+1$, $-x+1$, $-z+3/2$; #2, $x-1$, y, z. [b] #1, x, $-y+1/2$, $z+1/2$; #2, $-x+1$, $-y+1$, $-z$.

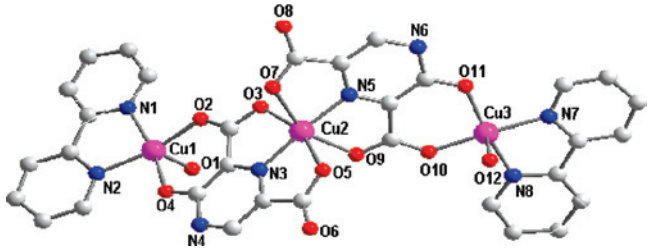

Figure 1. Coordination environment of Cu(II) ions in **1** drawn at 50% probability level. All hydrogen atoms and lattice−water molecules are omitted for clarity.

Scheme 2. Coordination Modes of the Ligands in **1**, **2**, and **4**

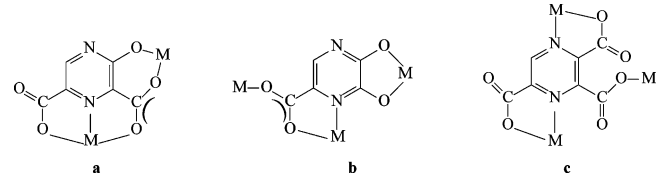

transformed to **INT3Cu** via a transition state **TS2Cu** with an activation energy barrier of ~25.0 kcal/mol, which is the rate determining step of the whole reaction.

After the formation of **INT3Cu**, extensive searches on the probable reaction pathways indicated that two competitive pathways could be explored and characterized, in which pathway **a** will lead to the crystal **1**(Figure 10) and pathway **b** will form the crystals **2** and **3**(Figure 11). Usually, it is improbable that attacking of OH^- on pyrazine ring results in the departure of a COO^- (S_N2 reaction). However, the reaction becomes accessible with the assistance of Cu^{2+}, in which the activation barrier was calculated to be ~0.2kcal/mol on going from **INT3Cu** to **COM2Cu** via **TS3Cu** in pathway **a**. As shown in Figure 10, **COM2Cu** will be transformed to crystal **1** through a few steps without any activation barrier. If a second OH^- continues to insert into **INT3Cu** through the transition state **TS4Cu**, crystals **2** and **3** will be formed through a more complicated process. As illustrated in Figures 11 and 12, the formation of **INT7Cu**

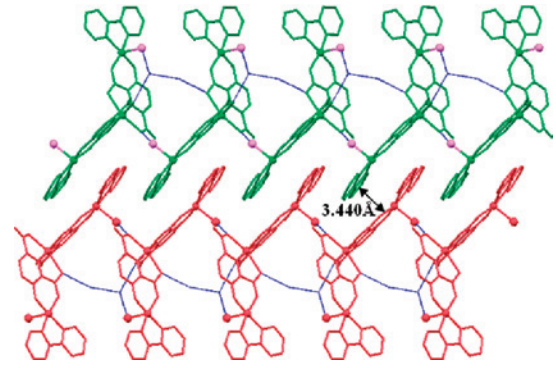

Figure 2. Supramolecular network of complex **1** containing hydrogen bonds and π-π stacking.

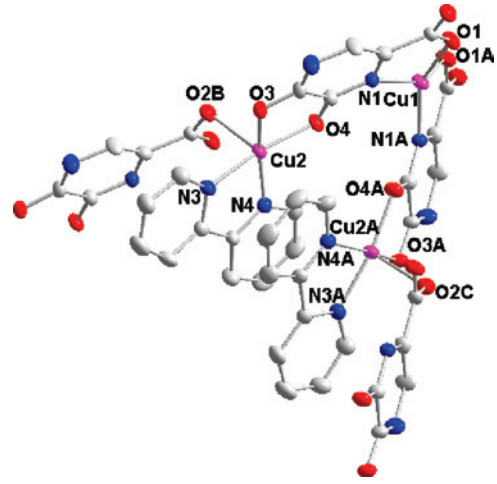

Figure 3. Coordination environment of Cu (II) ions in **2** drawn at 50% probability level. All hydrogen atoms are omitted for clarity.

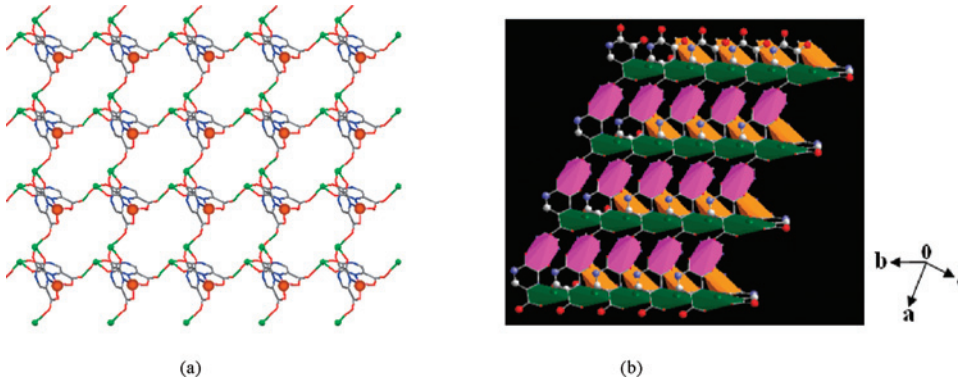

Figure 4. (a) 2D layer structure of **2** containing a 32-membered metallocycle along the *c*-axis. (b) Cu(II) ions as shown in polyhedra are located at different planes.

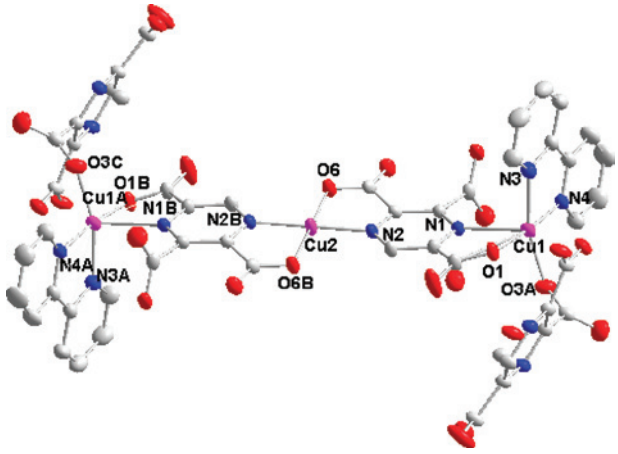

Figure 5. Coordination environment of Cu(II) ions in **4** drawn at 50% probability level. All hydrogen atoms and lattice−water molecules are omitted for clarity.

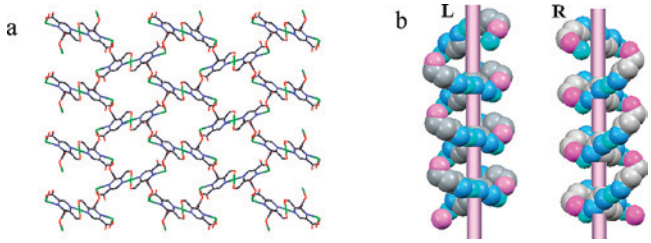

Figure 6. (a) 2D MOF of **4** along the *b*-axis; (b) the space-filling models of the left and right-hand helical chains.

from **INT3Cu** needs to overcome an about 2.8 kcal/mol energy barrier, indicating that this process can be easily accessible. However, the crystallization is a very complicated process, which is related to the concentration, temperature, and other conditions.

Obviously, the introduction of the OH^- ion would bring redundant electrons into the system, and this electron could be transferred to Cu(II), that is, the transformation of Cu^{2+} into Cu^+ helps to transfer the redundant electrons and plays an important role in the formation of complexes **1**−**3**. For example, with the insertion of OH^-, one of the Cu atoms in **COM1Cu**, **TS2Cu**, **INT3Cu**, **TS3Cu**, and **COM2Cu** should be a monovalent Cu(I) (see Table 3); however, they are oxidized back to Cu(II) in **INT6Cu** with the help of Cu^{2+}. In other word, both two Cu atoms in the final complex **1** should be Cu(II). This

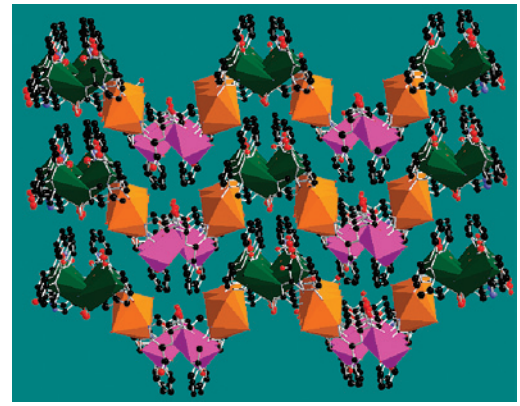

Figure 7. "W"-like 3D supramolecular network, the different colourful polyhedra represent the Cu(II) ions in different planes.

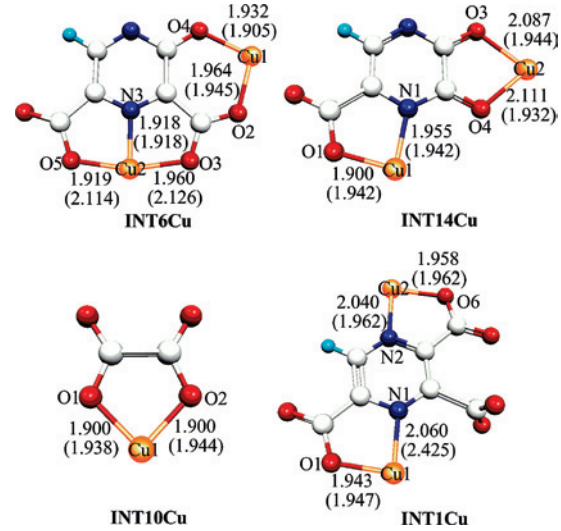

Figure 8. Comparison of selected optimized bond lengths (Å) relative to Cu atoms in the last structures leading to complexes **1**−**4**, with those obtained from the corresponding crystals in parentheses.

may explain why only solvable copper salts could help to form the complexes **1**−**3**mentioned above.

Magnetic Properties of the Complexes 1, 2, and 4. For complex **1**, the value of μ_{eff} at 300 K is 2.93 μ_B, slightly lower than the spin-only value (3.0 μ_B) expected for the magnetically isolated three $S = 1/2$ spins with $g = 2.0$. This value smoothly decreases upon cooling and gives a plateau around 30 K, corresponding to a value of 1.86 μ_B, which

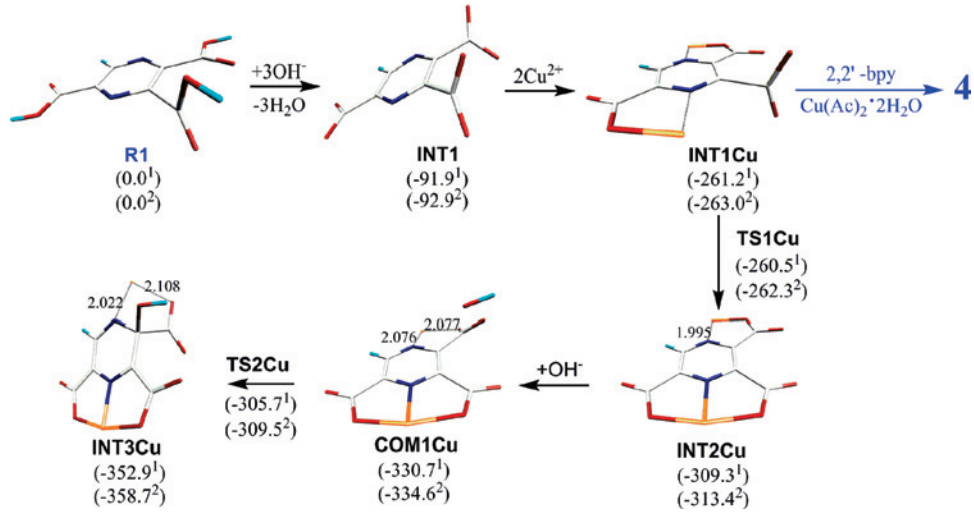

Figure 9. Reaction scheme and relative energies (energy in kcal/mol and bond lengths in Å) for the formation of complexes **4** and **INT3Cu**. (1) SCRF-UB3LYP/6−31+G(d) (Cu atom using a LanL2DZ basis set) in H_2O solution, with a 0.96 scaling factor for the ZPE correction.[17] (2) The same as 1 but without the ZPE correction.

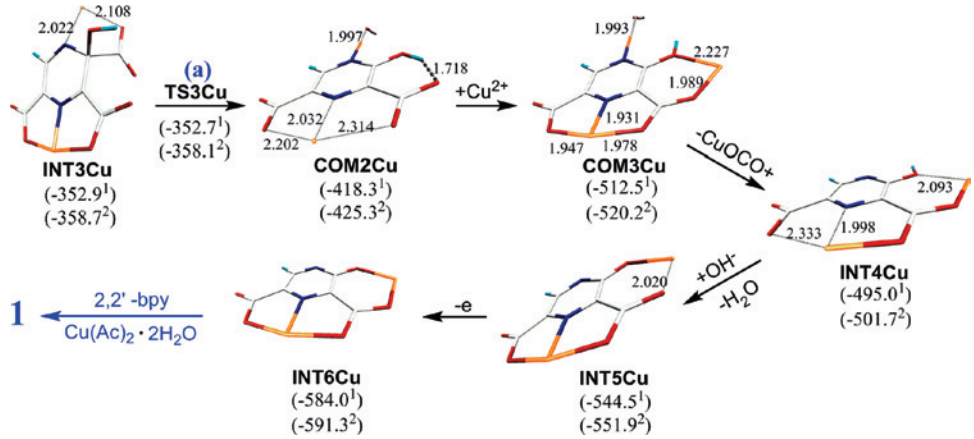

Figure 10. Reaction scheme and relative energies (energy in kcal/mol and bond lengths in Å) for the formation of complex **1**. (1) SCRF-UB3LYP/6−31+G(d) (Cu atom using a LanL2DZ basis set) in H_2O solution, with a 0.96 scaling factor for the ZPE correction.[17] (2) The same as 1 but without the ZPE correction.

indicates a spin doublet state. Further cooling below 5 K, a sudden decrease of the μ_{eff} value is observed, down to 1.63 μ_B at 2.0 K (Figure 13). The above features are typical of isolated trinuclear copper(II) species with strong antiferromagnetic coupling between Cu(II) ions.

To estimate the magnitude of the antiferromagnetic coupling, the magnetic susceptibility data were fitted to a trinuclear-copper(II) model. The Hamiltonian describing the situation of the trimer is given as $\hat{H} = -J(\hat{S}_1\hat{S}_2 + \hat{S}_2\hat{S}_3)$, where J is the exchange interaction between the central and terminal copper(II) ions. The expression of magnetic susceptibility, derived from the Hamiltonian, is given as

$$x_{tri} = \frac{Ng^2\beta^2}{4kT}\frac{1 + \exp[J/kT] + 10\exp[3J/2kT]}{1 + \exp[J/kT] + 2\exp[3J/2kT]}$$

Considering the weak interactions between trimer units, the susceptibility can be corrected by the mean-field, zJ'.[19]

$$\chi_M = \chi_{tri}/[1 - (zJ'x_{tri}/Ng^2\beta^2)]$$

The best fit to the experimental data leads to $g = 2.13$, $J = -99.27$ cm^{-1}and $zJ' = -1.20$ cm^{-1}, $R = 7.88 \times 10^{-4}$ (the R value is defined as $\sum[(\chi_M)_{obs} - (\chi_M)_{calc}]^2/\sum[(\chi_M)_{obs}]^2$).

As shown in Figure 14, the μ_{eff} value at the room temperature for **2** per trinuclear unit is equal to 3.25 μ_B, a value which is slightly higher than that expected for the spin-only value of 3.0 μ_B of three noninteracting copper(II) ions assuming $g = 2.00$. This value continuously decreases when the temperature is lowered and decreases abruptly below 25 K, reaching a value of 1.83 μ_B at 2 K. This behavior is an indication of the occurrence of antiferromagnetic interaction.

As indicated in the crystal structure, complex **2** is a two-dimensional copper(II) net bridged by ligand $DHPZA^{3-}$, in which the carboxylate group of $DHPZA^{3-}$ adopts a *syn-anti* fashion to link the Cu(2) and Cu(1A) in the equatorial-axial positions. As has been pointed out by Colacio et al.,[20] when carboxylate groups link copper(II) in *syn-anti* equatorial-axial positions, the coupling through the bridging ligand is always very small regardless of the structural parameter of the bridge. Therefore, from a magnetic point of view, complex **2** can be described as a trinuclear copper(II) complex bridged by $DHPZA^{3-}$ and the magnetic data are analyzed by means of the trinuclear model. Employing the same equations

(19) Oconnet, C. J. *Prog. Inorg. Chem.* **1982**, *29*, 203.
(20) Colacio, E.; Ghazi, M.; Kivekas, M.; Moreno, J. M. *Inorg. Chem.* **2000**, *39*, 2882.

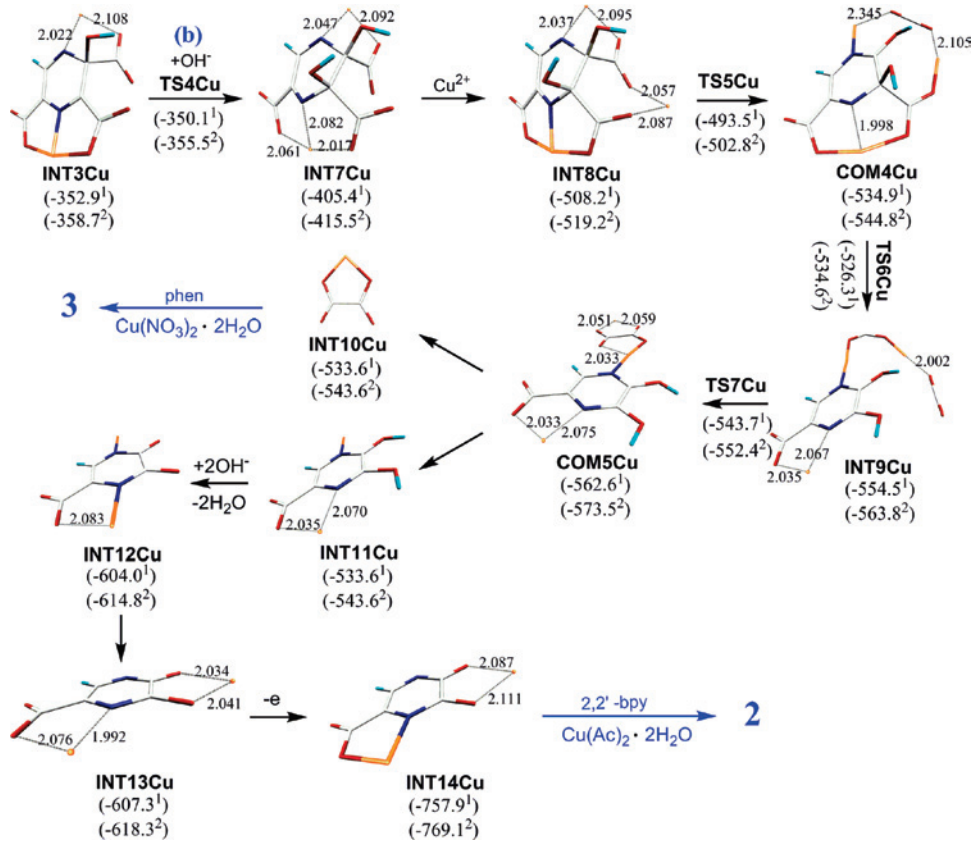

Figure 11. Reaction scheme and relative energies (energy in kcal/mol and bond lengths in Å) for the formation of complexes **2** and **3**. (1) SCRF-UB3LYP/6−31+G(d) (Cu atom using a LanL2DZ basis set) in H_2O solution, with a 0.96 scaling factor for the ZPE correction.[17] (2) The same as 1 but without the ZPE correction.

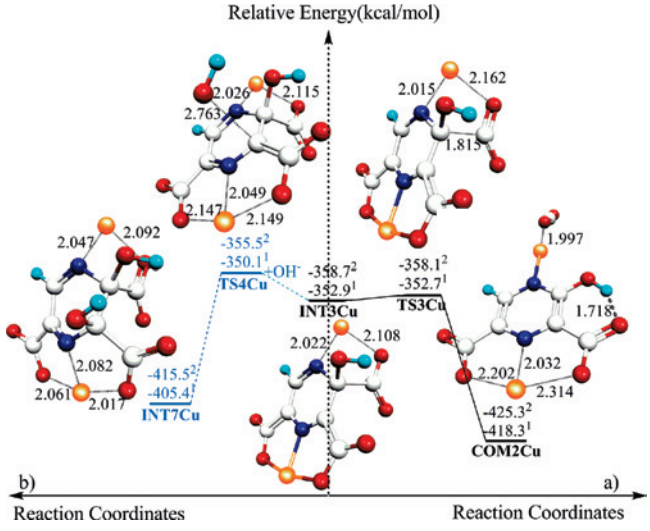

Figure 12. Part of the reaction potential energy surface (energy in kcal/mol and bond lengths in Å), along with the ball and stick models of the corresponding structures. (1) SCRF-UB3LYP/6−31+G(d) (Cu atom using a LanL2DZ basis set) in H_2O solution, with a 0.96 scaling factor for the ZPE correction. (2) The same as 1 but without the ZPE correction.

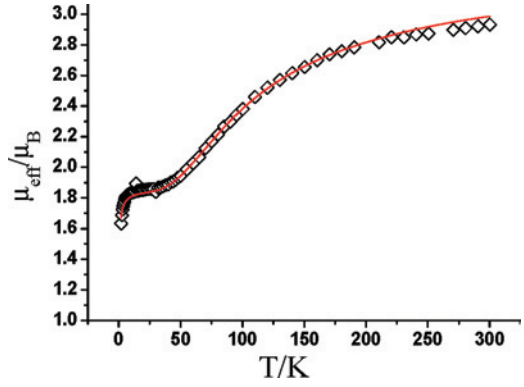

Figure 13. Plot of μ_{eff} versus T for **1**; the solid line represents the best theoretical fit.

Table 3. Calculated Mulliken Atomic Spin Density of Selected Stationary Points, Obtained at SCRF-UB3LYP/6-31+G(d) (Cu Atom Using a LanL2DZ Basis Set) in H_2O Solution

	COM1Cu	TS2Cu	INT3Cu	TS3Cu	INT6Cu
Cu1	+0.567	+0.553	+0.561	+0.555	+0.578
Cu2	−0.006	−0.004	+0.057	+0.028	+0.582

described above, the best fit to the experimental data gives $g = 2.14$, $J = -7.43$ cm^{-1} and $zJ' = -0.51$ cm^{-1}, $R = 1.49 \times 10^{-3}$ (the R value is defined as $\sum[(\chi_M)_{obs} - (\chi_M)_{calc}]^2/\sum[(\chi_M)_{obs}]^2$), where J is the exchange interaction between the central copper(II) (Cu(1)) and the terminal copper(II) (Cu(2),Cu(2A)) and zJ' is a weak interaction transferred by the *syn-anti* carboxylate bridges.

For complex **4**, the room temperature μ_{eff} value per trinuclear unit is 3.37 μ_B, larger than the spin-only value expected for a magnetically isolated trinuclear copper(II) with $g = 2.00$. Upon cooling, the μ_{eff} value gradually decreases and reaches 3.14 μ_B at 2.0 K. The variation χ_M with T obeys the Curie−Weiss law as there is a linear relationship between $1/\chi_M$ and T. The corresponding Curie constant (C) and Weiss constant (θ) are found to be 1.41

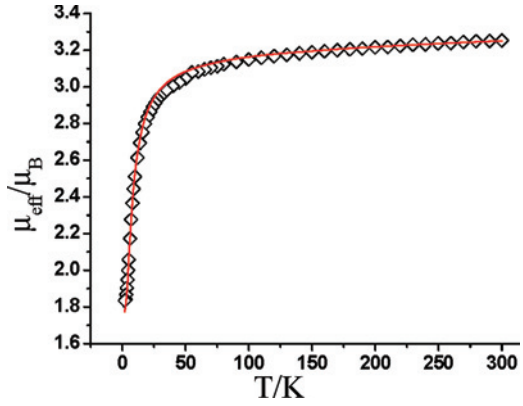

Figure 14. Plot of μ_{eff} versus T for **2**; the solid line represents the best theoretical fit.

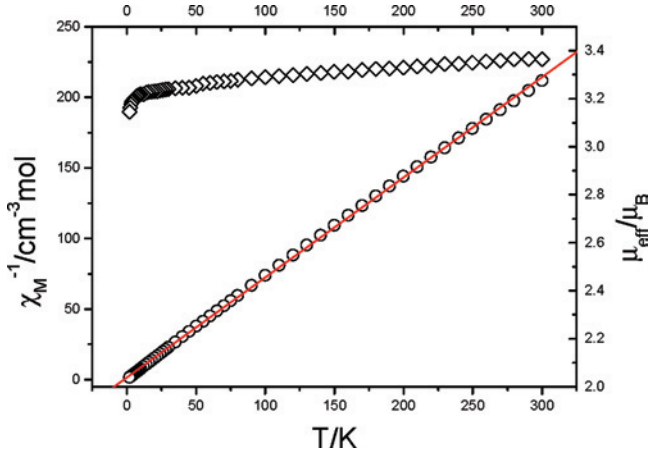

Figure 15. Plots of μ_{eff} (◇) and χ_M^{-1}(○) versus T for **4**; the solid line represents the best theoretical fit.

cm^3 K mol^{-1} and −2.06 K, respectively. The small negative θ value indicates that a very weak antiferromagnetic interaction is operative between neighboring copper(II) ions, as shown in Figure 15.

The fitting results indicate that the magnitude of the magnetic coupling between the adjacent copper(II) ions in **1**, **2**, and **4** is very different. This may be attributed to the different structures. For complex **1**, the coordination around two terminal copper(II) ions are 4 + 1; thus, the magnetic orbitals at Cu(1) and Cu(3) are the $d_{x^2} - y^2$ type lying in the basal planes, whereas that is d_{z^2} type for central copper(II) because of the compressed octahedral geometry of Cu(2) toward to N(3) and N(5). According to the structural data, the planar bridging ligand is approximately coplanar to the basal plane of the terminal metal and links neighboring copper(II) ions by equatorial−equatorial and axial modes. This results in a better overlap of the two magnetic orbitals and produces a strong antiferromagnetic interaction as observed. For complex **2**, the magnetic orbital at each copper(II) ion is mainly of $d_{x^2} - y^2$ type lying in the basal plane, with a small contribution from d_{z^2}, and the superexchange coupling is mediated through the ligand DHPZA^{3-}. However, the overlap between the magnetic orbitals of Cu(1) and Cu(2) is poor because of the strongly distorted square-planar geometry around Cu(1), and the resulting magnetic exchange is weak. For complex **4**, it shows a 2D copper(II) layer. In this layer, there are two pathways to mediate magnetic coupling between the copper(II) ions, namely, (i) interaction transmitted by PZTC^{3-} through the bibidentate pathway (N(1)O(1)—N(2)O(6)) (J) and (ii) magnetic coupling through the monobidentate pathway (O(3)—N(1)O(1)) (J'). As known, the bridging ligand can transfer magnetic exchange interactions through σ as well as π pathways, and a linker with only σ-bonding is a significantly weaker mediator.[21] For the second magnetic pathway in **4**, the delocalized π system is destroyed because the plane of the carboxylate (C(6)O(3)O(4)) almost is perpendicular (85.0°) to the plane of pyrazine ring; thus, the magnetic coupling transferred by this pathway should be very weak. For the first magnetic pathway, there it can be seen that the basal planes of Cu(1) and Cu(2) are nearly orthogonal (dihedral angle of 94.7°) and that the out-of-plane exchange pathway is involved. This results in the significantly reduced overlap of the magnetic orbitals and a very weak antiferromagnetic interaction between Cu(1) and Cu(2) in **4**.[22,23]

Conclusion

Four copper complexes were synthesized under Cu(II)/H_3PZTC hydrothermal reaction conditions at different temperature and/or pH and characterized by single-crystal X-ray diffraction. The results show that the higher temperature and pH favor the in situ Cu(II)/H_3PZTC hydrothermal reactions, in which H_3PZHD and H_3DHPZA can be obtained while they could be hardly carried out in organic synthesis. The formation mechanism of the complexes **1**−**4** has been characterized with DFT calculations, indicating that electron transfer between OH^- and Cu^{2+} and redox of Cu^{2+}/Cu^+ play an important role in the in situ Cu(II)/H_3PZTC hydrothermal reactions. This assumption can possibly be used for explaining why in many in situ metal/ligand hydrothermal reactions the metal is a Cu(II) ion,[3,5c,6,8] and thus new organic compounds can be prepared by the in situ Cu(II)/ligand hydrothermal reactions. This topic is promising.

Acknowledgment. This work was supported by the National Natural Science Foundation of China (Nos. 20331010, 20501003, and 20773016). D.C.F. thanks the program NCET(NCET-04-0146), MSSBRD(2004CB719903), and High-powered computing center of Beijing Normal University for partial CPU time.

Supporting Information Available: Crystallographic files in cif format. Tables S1−S3 with optimized coordinates, frequencies, and energies of complexes **1**−**4**; Figures S1, S2 containing properties of complex **4** (PDF). This material is available free of charge via the Internet at http://pubs.acs.org.

IC8001916

(21) (a) Galán-Mascarós, J. R.; Dunbar, K. R. *Angew. Chem., Int. Ed.* **2003**, *42*, 2289. (b) Day, P. *J. Chem. Soc., Dalton Trans.* **1997**, 701.
(22) (a) Kahn, O. *Angew. Chem., Int. Ed. Engl.* **1985**, *24*, 834. (b) Verdaguer, M. *Polyhedron* **2001**, *20*, 1115. (c) Ruiz-Pérez, C.; Sanchiz, J.; Molina, M. H.; Lloret, F.; Julve, M. *Inorg. Chem.* **2000**, *39*, 1363.
(23) (a) Julve, M.; Verdaguer, M.; Faus, J.; Tinti, F.; Moratal, J.; Monge, A.; Gutiérrez-Puebla, E. *Inorg. Chem.* **1987**, *26*, 3520. (b) Zheng, L. M.; Wang, Y. S.; Wang, X. Q.; Korp, J. D.; Jacobson, A. J. *Inorg. Chem.* **2001**, *40*, 1380.